Electronic Structure of Passivated $Au_{38}(SCH_3)_{24}$ Nanocrystal

H. Häkkinen, R. N. Barnett, and U. Landman
School of Physics, Georgia Institute of Technology, Atlanta, Georgia 30332
(Received 15 December 1998)

Energetics, electronic structure, charging, and capacitive properties of bare and thiol-passivated Au_{38} gold nanocrystals were investigated via density-functional calculations. In the energy-optimized passivated nanocrystal, comprised of a truncated-octahedral face-centered-cubic Au_{38} core coated by a monolayer of 24 methylthiol (SCH_3) molecules, we find interfacial charge transfer of about $2e$ from the outermost gold atoms to the sulfur atoms. The estimated effective capacitance is 0.084 aF, correlating well with recent electrochemical measurements. Charging takes place within the molecular layer. Molecular adsorption of dimethyl-disulfide is found to be energetically unfavorable for a gold cluster of this size. [S0031-9007(99)08937-1]

PACS numbers: 36.40.Cg, 36.40.Mr, 61.46.+w

Gold-containing nanometer-sized structures are currently under intensive study in a wide variety of areas, including colloidal chemistry [1], catalysis [2], medical science [3], and cluster science [4–8]. Quite recently, it has been shown that it is possible to prepare and isolate quantitatively a discrete family of mass-selected fractions of gold nanoparticles passivated by a monolayer of thiol molecules (R-SH, with $R = (CH_2)_nCH_3$) [4,8]. Moreover, these nearly monodispersed fractions, with the core-gold sizes corresponding to structures of enhanced ("magic") energetic stability [4,6], can be used for assembly of two- and three-dimensional superlattices. Such structures possess interesting transport and spectroscopic properties which are expected to be useful in applications to nanocircuits, optoelectronics, and sensor technologies [9].

While the detailed atomistic structure and morphology of the above-mentioned gold core clusters with effective diameters ranging from 1 to 2 nm (14 to 40 kDa in mass, 1 kDa corresponds to the mass of approximately five Au atoms) have been recently resolved through theoretical molecular dynamics modeling coupled with x-ray powder diffraction analysis [6], little is known theoretically about their electronic structure, particularly pertaining to the nature and the effect of the Au-S interaction at the interface between the metal core and passivating molecules.

This Letter reports on a density-functional study of one of the smallest alkylthiol-passivated gold nanoparticles (8 kDa Au core mass) successfully isolated in large quantities in solutions [7,8], investigating its energetics, structure, electronic spectrum, charging, and capacitive properties. We show that passivation of the gold crystallite, i.e., to form $Au_{38}(SCH_3)_{24}$, is accompanied by an internal charge transfer from the outermost gold atoms to the surrounding adsorbed sulfur atoms, and that the integrated charge deficit in the gold core is about $2e$. Charging (removing or adding electrons) changes the spatial charge density almost exclusively in the molecular layer. Considering the nanoparticle as a quantum dot, the effective capacitance is estimated to be 0.084 aF (1 aF = 1×10^{-18} F), correlating well with recent electrochemical measurements [7].

The calculations are done using the density-functional pseudopotential plane-wave method [Born-Oppenheimer local-spin-density (LSD) molecular dynamics] [10], recently rewritten for massively parallel computing. The valence electrons [11, 6, 4, and 1 for Au, S, C, and H, respectively, i.e., $418e$ in the bare Au_{38} cluster and $730e$ in the $Au_{38}(SCH_3)_{24}$] are described by norm-conserving nonlocal pseudopotentials [11] with a plane-wave basis set (kinetic energy cutoff of 62 Ry) [12].

According to recent molecular dynamics investigations of bare gold clusters [6], which used the embedded atom potential (EAM), the energetically most favorable structure for the Au_{38} cluster is face-centered-cubic with a truncated octahedral morphology. In this structure, there is a regular six-atom octahedron centered about the origin, with an interatomic distance of 2.82 Å. The distance from these inner atoms to the surface atoms (32) is 2.67 Å, and the interatomic distance between nearest-neighbor surface atoms is 2.72 Å. The surface consists of six (100) facets and eight (111) facets.

Starting from the EAM optimal configuration of the cluster, full (unconstrained) local-density approximation (LDA) relaxation introduces only minor changes to the structure (see inset of Fig. 1a): The eight atoms in the middle of the (111) facets displace slightly outwards to make the cluster more spherical, and as a result all of the interatomic distances become more uniform falling in the range of 2.74–2.78 Å.

We passivate the cluster by 24 methylthiol SCH_3 molecules, symmetrically positioned on the (111) facets close to the (111)/(100) edges. The chosen ratio (24/38) between the number of molecules and Au atoms agrees with the experimentally resolved elemental composition of the 8 kDa $Au:SC_6$ cluster material [17]. In the optimized structure of the passivated crystal, shown in the inset of Fig. 1b, we note a general outward relaxation of the six-atom inner octahedron and the 24 corner surface

 0031-9007/99/82(16)/3264(4)$15.00

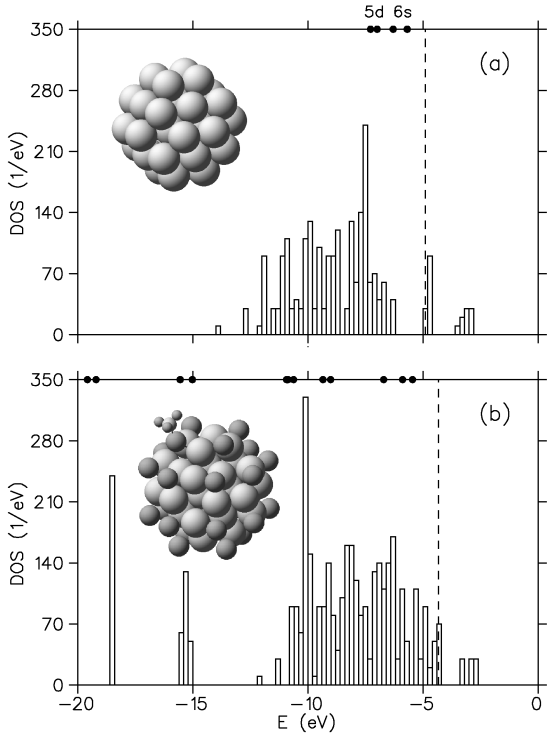

FIG. 1. Density of Kohn-Sham states (DOS) of the (a) Au_{38} cluster and (b) passivated $Au_{38}(SCH_3)_{24}$ cluster. The dots on the upper axes denote the eigenenergies of (a) Au atomic valence states, and (b) SCH_3 molecular valence states. The dashed line denotes the Fermi energy. The width of the energy bins is 0.2 eV. The insets in (a) and (b) show the optimized structures of the bare gold and the passivated clusters, respectively. In (b) the sulfur atoms are depicted as darker spheres and only one CH_3 group is shown.

gold atoms, with their interatomic distances increased to 2.95–2.97 Å. The eight atoms in the middle of the (111) facets are now relaxed inwards with respect to the facet edges. The Au-S, S-C, and C-H distances are 2.52, 1.87, and 1.10 Å, respectively, with an Au-S-C angle of 126°.

The densities of Kohn-Sham levels (DOS) for the bare and passivated Au_{38} clusters are shown in Figs. 1a and 1b, respectively. The DOS of Au_{38} features a threefold degenerate highest occupied molecular orbital (HOMO) state (six states including spin, four of them occupied leaving two holes) due to the octahedral symmetry [18]. Furthermore, there is a set of 18 empty states (including spin) just above the Fermi level, and gaps of 1.3 and 1.1 eV *below* and above the Fermi level. We note that the total width of the valence band (≈9 eV) is already close to the one of bulk fcc gold [19], but the finite size of the cluster results in a gap below the Fermi level (bulk gold has a very low DOS in this region). The orbital characters of the HOMO states (i.e., at the Fermi level) show significant s, p, and d hybridization as follows: (i) for the six-atom inner octahedron $s(0.42)$, $p(0.13)$, $d(0.45)$; (ii) for the eight atoms in the middle of the (111) facets $s(0.003)$, $p(0.28)$, $d(0.71)$, $f(0.004)$; and (iii) for the 24 corner atoms [of the six (100) facets] $s(0.20)$, $p(0.21)$, $d(0.57)$, $f(0.01)$; with the values in parentheses giving the relative weights of the corresponding angular momentum states, obtained via averaging the local spherical-harmonics decomposition of the HOMO states on each atom in the respective region.

The most prominent features in the DOS of the passivated cluster are (i) the two narrow "bands" at about −18.5 and −15.2 eV, formed from the SCH_3 molecular orbitals, (ii) the upward shift of the gold states by 1.8 eV, (iii) the filling of the gap below the Fermi energy, and (iv) the significant reduction in the number of holes at, and just above, the Fermi energy (the number of empty states including spin reduces to six). The gap above the Fermi level is 0.9 eV, coinciding with that measured through optical absorbance spectroscopy [7]. In the passivated cluster, the HOMO state remains threefold degenerate, and a spatial analysis of its orbital charge density reveals that it is concentrated around the outermost 24 gold atoms and the surrounding 24 sulfur atoms, having a d character on the gold atoms and a p character on the sulfurs.

We now turn to a discussion of the charge transfer and charging properties of the passivated gold nanocrystal. In Fig. 2a, we display the radial electron density difference, $4\pi R^2\Delta\rho(R)$, where $\Delta\rho = \rho(\mathrm{Au_{38}(SCH_3)_{24}}) - [\tilde{\rho}(\mathrm{Au}) + \tilde{\rho}(\mathrm{(SCH_3)_{24}})]$, where the "subsystem" densities $\tilde{\rho}$ are separately evaluated for the gold core and molecular layer (in the configuration of the optimal passivated cluster). $\Delta\rho$ shows that the electron-density deficit and buildup regions concentrate around the outermost 24 gold atoms and the 24 sulfur atoms, respectively (see Figs. 2a

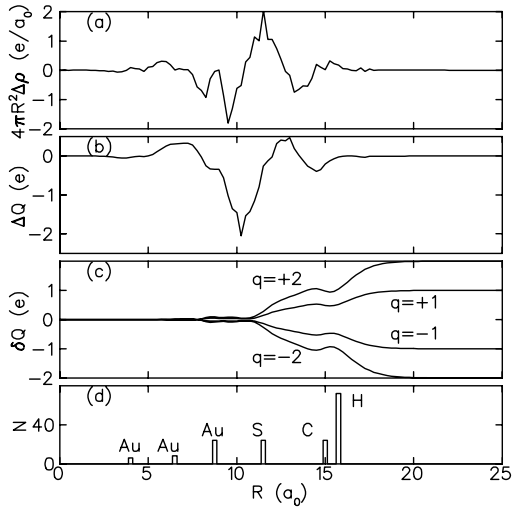

FIG. 2. (a) Radial electron density difference $4\pi R^2\Delta\rho(R)$ (see text for definition) for the relaxed passivated nanocrystal. (b) The integral $\Delta Q(R)$ of (a). (c) Integrated electron density difference between the neutral and charged passivated cluster $\delta Q(R) = 4\pi \int^R R'^2[\rho^0(R') - \rho^q(R')]\,dR'$, with $-2 \le q \le +2$, as marked on the figure; ρ^0 denotes the density for the neutral cluster. (d) Radial distribution of atoms, N, calculated from the center of mass of the nanocrystal. Distance in units of Bohr radius, a_0.

and 2d). The integral $\Delta Q(R) = \int^R \Delta\rho(R')\,dR'$, plotted in Fig. 2b, shows that the charge deficit in the gold core amounts to about two electrons by the midpoint between the outermost gold and sulfur atoms. This charge transfer also explains the aforementioned expansion of the gold core due to the increased interionic Coulomb repulsion. The charge transfer from gold to sulfur can be expected, since the elemental dimer AuS and trimer Au_2S are strongly polar (our calculation results in a dipole moment of 2.15 and 2.41 debye, respectively) [13].

Figure 2c shows the difference in the integrated charge between the neutral and charged cluster, $\delta Q(R)$. Surprisingly, the addition/removal of extra charge takes place almost exclusively *within the molecular layer*. This result, combined with the observed intracluster charge transfer, indicates that charging of passivated metal nanocrystals may lead to more complex spatial charge patterns than has commonly been expected.

Calculated first and second vertical ionization potentials and electron affinities are given in Table I. Our results for the bare Au_{38} cluster agree well with quantum chemical LDA/GGA (generalized gradient approximation) calculations [20], and our calculated EA is in reasonable agreement with the measured one [21] ($\approx$3.8 eV). Passivation results in significantly lower IP, IP2, and EA values, but increases EA2.

Since potential applications of passivated metal nanocrystals include their use as elements in nanocircuit devices, it is of interest to assess theoretically their capacitive properties. By analogy to quantum dots, a high enough addition energy can lead to (room-temperature) Coulomb blockade effects in electron transport through such nanocrystals. The addition energy [22] can be expressed as the discrete second derivative of the total energy with respect to number of electrons N_e,

$$E_{\text{add}} = E(N_e + 1) - 2E(N_e) + E(N_e - 1) = \Delta\epsilon + e^2/C\,, \quad (1)$$

and using a simple model [22], E_{add} consists [see second equality in Eq. (1)] of the change in the single-electron energy $\Delta\epsilon = \epsilon(N_e + 1) - \epsilon(N_e)$ of the highest occupied level and the charging energy e^2/C which defines the effective capacitance C of the quantum dot. Hence, for the neutral cluster ($N_e = N_e^0$) the simple relation $E_{\text{add}} = \text{IP} - \text{EA}$ holds. Taking into account the fact that in going from charge state $q = -2$ to $+2$ the added electron(s) is filling the holes in a degenerate set of levels (see discussion of Fig. 1b), $\Delta\epsilon \approx 0$ in Eq. (1), and the effective capacitance is determined simply by the charging energy. Taking $N_e = N_e^0 \pm 1$ in Eq. (1), we arrive at an estimate of 0.084 ± 0.001 aF for C [from both LSD and post-xcg calculations; similarly, our estimate for C of the bare Au_{38} cluster is 0.066 ± 0.001 aF]. This in turn implies that there is a constant shift of about 1.9 eV of all the eigenvalues due to charging. Indeed, the observed shifts of the HOMO eigenvalue are in the range of 1.90 to 1.92 eV and the shifts of the lowest eigenvalues are 1.81 to 1.84 eV (that is, charging induces a rigid, uniform, shift of the eigenvalue spectrum).

TABLE I. Calculated first and second ionization potentials (IP, IP2) and electron affinities (EA, EA2) for the bare and passivated Au_{38} clusters. BE is the binding energy per gold atom in Au_{38} and the binding energy per SCH_3 molecule in $Au_{38}(SCH_3)_{24}$. The two values given for our calculations correspond to results from LSD/post-xcg calculations and those quoted from Ref. [19] correspond to LDA/GGA results. All energies are in eV.

	Au_{38} This study	Au_{38} Ref. [19]	$Au_{38}(SCH_3)_{24}$ This study
IP	6.14/5.75	6.31/6.07	5.31/5.18
IP2	8.62/8.23		7.23/7.11
EA	3.70/3.33	3.86/3.67	3.41/3.27
EA2	1.29/0.91		1.45/1.32
BE	3.29/2.12	3.44/2.35	2.19/1.39

Recently, Chen *et al.* [7] performed Coulomb staircase measurements on solutions of gold nanoparticles with Au core sizes of 8 to 38 kDa. In this experiment, an effective capacitance was determined for an "electrochemical ensemble" of clusters of a certain core mass, i.e., for those (large number of) clusters that become charged in the vicinity of the metal electrode/solution interface and depart/reach the electrode by diffusion. The effective capacitance for the passivated 8 kDa (i.e., Au_{38}) cluster was determined to be 0.13 aF. While our estimate falls below the experimental value, the comparison between the two is rather satisfactory in view of several factors not addressed in our calculations; these include a thicker molecular layer, i.e., the effect of longer carbon chains (in the experiments hexanethiol was used for coating of the 8 kDa cluster), and local polarization effects around the cluster in solution. Both of these effects would tend to increase our calculated value for C.

Finally, we wish to comment on an ongoing discussion pertaining to the structure of the gold-substrate–sulfur-headgroup interface in self-assembled monolayers on Au(111). The "traditional" picture of Au-thiolate bonding [23] has been recently challenged [24,25] by interpretations of x-ray and STM results which suggest dimerization of the sulfur headgroups. The most recent adsorption model of decanethiols on the Au(111) surface [25] has some relevance to our study, since it suggests a sulfur pairing model where one of the sulfur atoms (S1) is laterally within 0.5 Å of a gold atom atop site at a vertical height $h_1 = 2.21$ Å, with the other sulfur (S2) being in an annulus surrounding a hollow site with $h_2 = 2.97$ Å, d(S1-S2) = 2.3 Å, and the S1-S2 bond tilted 19° away from the surface plane. The seven-atom (111) facet of our Au_{38} cluster is the smallest one that could accommodate this structure. A full relaxation for $Au_{38}(H_3CS\text{-}SCH_3)$ starting from the above-mentioned configuration leads indeed to a local

minimum molecular adsorption state, where S1 is bonded directly in an atop site, with $h_1 = 2.65$ Å, $h_2 = 3.25$ Å, d(S1-S2) = 2.11 Å, and a tilt angle of 10°. However, dissociation of the dimethyl-disulfide molecule and adsorption of the two separate SCH_3 molecules on two nonadjacent Au-Au bridges on the (111) facet is found to be energetically more favorable (with an energy advantage of at least 1.6 eV per H_3CS-SCH_3 molecule, calculated via LDA with post-xcg corrections). While this result suggests that molecular adsorption of dimethyl-disulfide on a gold cluster of this size is energetically unfavorable, further investigations of this issue are certainly warranted, particularly on larger gold clusters [which have more extended (111) facets] and for longer thiols.

In summary, we have presented a first theoretical investigation to examine in detail the geometric and electronic structure of passivated metal nanocrystals, using the $Au_{38}(SCH_3)_{24}$ cluster as a case study. Our results show significant intracluster charge transfer at the metal-core–molecular-layer interface and unveils spatial charging and energetic patterns that we expect to prove useful for future efforts to understand the rapidly accumulating experimental data on these systems.

This research is supported by the DOE and AFOSR. The computations have been done mainly on IBM SP2 at the GIT Center for Computational Materials Science, and at the National Energy Research Scientific Computing Center (NERSC), Berkeley, California. We gratefully acknowledge the most helpful contribution of A. Canning (NERSC) to the development of the parallel computer code, and thank C. L. Cleveland, W. D. Luedtke, and R. L. Whetten for useful discussions.

[1] *Colloidal Gold: Principles, Methods, and Applications*, edited by M. A. Hayat (Academic Press, San Diego, 1991).
[2] D. A. H. Cunningham *et al.,* J. Catal. **177**, 1 (1998).
[3] R. C. Elder *et al.,* J. Am. Chem. Soc. **107**, 5024 (1985), and references therein.
[4] R. L. Whetten *et al.,* Adv. Mater. **8**, 428 (1996).
[5] W. D. Luedtke and U. Landman, J. Phys. Chem. **100**, 13 323 (1996).
[6] C. L. Cleveland *et al.,* Phys. Rev. Lett. **79**, 1873 (1997); C. L. Cleveland *et al.,* Z. Phys. D **40**, 503 (1997).
[7] S. Chen *et al.,* Science **280**, 2098 (1998).
[8] M. M. Alvarez *et al.,* Chem. Phys. Lett. **266**, 91 (1997); T. G. Schaaff *et al.,* J. Phys. Chem. **101**, 7885 (1997).
[9] C. P. Collier *et al.,* Science **277**, 1978 (1997).
[10] R. N. Barnett and U. Landman, Phys. Rev. B **48**, 2081 (1993).
[11] N. Troullier and J. L. Martins, Phys. Rev. B **43**, 1993 (1991). The pseudopotentials' core radii (in units of a_0) are as follows (tilde indicates local component): Au: $\tilde{s}(2.50)$, $p(3.00)$, $d(2.00)$; S: $s(1.80)$, $\tilde{p}(2.30)$; C: $s(1.50)$, $\tilde{p}(1.54)$; H: $\tilde{s}(0.95)$. The Au pseudopotential is relativistic and has been weight averaged by the j degeneracy of the $\ell \pm \frac{1}{2}$ states [see L. Kleinman, Phys. Rev. B **21**, 2630(1980); G. B. Bachelet and M. Schlüter, Phys. Rev. B **25**, 2103 (1982)].
[12] The adequacy of the pseudopotentials was tested separately for each atomic species, for elemental Au clusters up to Au_8, and for interelemental molecules, yielding good agreement with experimental data [13]. These tests included LDA/LSD calculations [14], without and with exchange-correlation gradient (xcg) corrections [15]. While the inclusion of gradient corrections improves the energetics in most cases (with self-consistent GGA and post-xcg [10,16] yielding close results), they were not found to change any of the observed trends, allowing us to safely resort to the use of the LSD approximation (with post-xcg corrections) for the larger bare Au_{38} and passivated $Au_{38}(SCH_3)_{24}$ nanocrystals.
[13] H. Häkkinen, R. N. Barnett, and U. Landman (unpublished).
[14] S. H. Vosko, L. Wilk, and M. Nusair, Can. J. Phys. **58**, 1200 (1980); S. H. Vosko and L. Wilk, J. Phys. C **15**, 2139 (1982).
[15] A. D. Becke, Phys. Rev. A **38**, 3098 (1988); J. Chem. Phys. **96**, 2155 (1992); J. P. Perdew, Phys. Rev. B **33**, 8822 (1986); **34**, 7046 (1986).
[16] C. Massobrio *et al.,* J. Chem. Phys. **109**, 6626 (1998).
[17] A sample of 8 kDa Au:SC_6 material has been determined, by x-ray photoemission spectroscopy, to have an elemental composition of 62% Au and 38% S. For 38 Au atoms this gives 23–24 thiol groups. [J. T. Khoury and R. L. Whetten (private communication)].
[18] In our calculations, we use a Fermi function with a temperature of 160 K (corresponding to 0.0136 eV) to determine the occupation numbers of the Kohn-Sham levels [10]. Consequently, the fact that in our unconstrained optimization the HOMO state remains degenerate means that any Jahn-Teller distortion resulting in splitting of the degeneracy by more than 0.0136 eV does not occur and the optimal structure determined by us is vibrationally stable, as we indeed verified via a short molecular dynamics simulation at 50 K.
[19] D. A. Papaconstantopoulos, *Handbook of the Band Structure of Elemental Solids* (Plenum Press, New York, 1986); A. H. MacDonald *et al.,* Phys. Rev. B **25**, 713 (1982); S. Bei der Kellen and A. J. Freeman, Phys. Rev. B **54**, 11 187 (1996).
[20] O. D. Häberlen *et al.,* J. Chem. Phys. **106**, 5189 (1997).
[21] K. J. Taylor *et al.,* J. Chem. Phys. **96**, 3319 (1992).
[22] L. P. Kouwenhoven *et al.,* in *Mesoscopic Electron Transport*, edited by L. L. Sohn *et al.* (Kluwer, Dordrecht, 1997), p. 105.
[23] C. D. Bain *et al.,* Langmuir **5**, 723 (1989); R. G. Nuzzo *et al.,* J. Am. Chem. Soc. **109**, 733 (1987); H. A. Biebuyk and G. M. Whitesides, Langmuir **9**, 1766 (1993).
[24] P. Fenter, A. Eberhardt, and P. Eisenberger, Science **266**, 1216 (1994); L.-J. Wan *et al.,* J. Phys. Chem. **102**, 5943 (1998).
[25] P. Fenter *et al.,* Surf. Sci. **412–413**, 213 (1998).